*Journal of the European Ceramic Society* **18** (1998) 1707–1710
© 1998 Elsevier Science Limited
Printed in Great Britain. All rights reserved
PII: S0955-2219(98)00096-X
0955-2219/98/$—see front matter

# Chemical Compatibility of $RE_{1-x}Sr_xMnO_{3\pm\delta}$ (RE = La, Pr, Nd, Gd, $0\leq x\leq 0{\cdot}5$) with Yttria Stabilized Zirconia Solid Electrolyte

G. Ch. Kostogloudis and Ch. Ftikos*

Laboratory of Inorganic Materials Technology, Department of Chemical Engineering, National Technical University of Athens, 9 Heroon Polytechniou Str., Zografou Campus, GR-157 80 Athens, Greece

(Received 24 December 1997; accepted 11 March 1998)

***Abstract***

*The chemical reactivity of $RE_{1-x}Sr_xMnO_{3\pm\delta}$ (RE = La, Pr, Nd, Gd) perovskite oxides with yttria stabilized zirconia (YSZ) was investigated. Equimolar perovskite/YSZ powder mixtures were prepared and annealed in air at 1300°C for 120 h. The X-ray diffraction analysis showed the formation of $RE_2Zr_2O_7$ and $SrZrO_3$ reaction products for perovskites with low and high Sr-content, respectively. Small amounts of $Mn_3O_4$ were identified for samples that showed high reactivity with YSZ. The extent of $RE_2Zr_2O_7$ formation is reduced as the ionic radius of the rare earth cation decreases, the only exception being $La_2Zr_2O_7$, which is formed in minor amounts. The formation of $SrZrO_3$ is favored with increasing Sr-content and decreasing tolerance factor of the perovskite. Among the compositions studied, $La_{1-x}Sr_xMnO_{3\pm\delta}$ showed the best chemical compatibility with YSZ electrolyte.*

## 1 Introduction

$La_{1-x}Sr_xMnO_{3\pm\delta}$ perovskite oxides are of great technological importance, since they are widely accepted as solid oxide fuel cell (SOFC) cathode materials. An issue of high importance for the successful operation of the cell is the chemical compatibility between the cathode and yttria stabilized zirconia (YSZ) solid electrolyte. The main reaction products reported in the literature[1–3] are $La_2Zr_2O_7$ and $SrZrO_3$, for low and high Sr-containing compositions, respectively. These products are formed during the high temperature heat treatment for the fabrication of the cell, and during its long term operation. Both products show lower electrical conductivities than YSZ,[4] and therefore their presence in the cathode/electrolyte interface is undesirable.

Although the chemical compatibility of La manganites with YSZ has been widely investigated, little information is available concerning the compatibility of other rare earth manganites. The investigation of their reactivity with YSZ attracts interest, since there are results in the literature[5] reporting that alternative rare earth manganite compositions exhibit higher electrical conductivity and lower overpotential values than those exhibited by lanthanum manganites. The purpose of the present work is, therefore, the comparative investigation of the chemical compatibility of $RE_{1-x}Sr_xMnO_{3\pm\delta}$ (RE = La, Pr, Nd, Gd) perovskite oxides with YSZ electrolyte.

## 2 Experimental

All $RE_{1-x}Sr_xMnO_{3\pm\delta}$ (RE = La, Pr, Nd, Gd) perovskite oxide powders were prepared by the citrate synthesis method.[6] $RE_2O_3$ was dissolved in $HNO_3$, while $Sr(NO_3)_2$ and $(CH_3COO)_2Mn{\cdot}4H_2O$ were dissolved in $H_2O$, all in the correct molar proportions. The solutions were mixed together and citric acid was added to bind all the metals. The final solution was heated over a burner flame, until combustion and pyrolysis took place. The obtained powders were calcined at 1100°C for 15 h, and wet milled with acetone using zirconia balls. The samples for the chemical compatibility tests were prepared by mixing equimolar amounts of perovskite and commercial YSZ (90 mol% $ZrO_2$) powders in an agate mortar, using acetone. The mixtures were

---

*To whom correspondence should be addressed.

subsequently compacted in pellets by uniaxial pressing at 250 MPa. The pellets were sintered in air at 1300°C for 120 h, and then milled and examined by X-ray powder diffraction. A SIEMENS diffractometer was used ($CuK_\alpha$ radiation) operated at 40 kV and 30 mA. The XRD data were collected by step scanning in the range $10 \leq 2\theta \leq 80$ in increments of 0·02° $2\theta$.

## 3 Results

The XRD patterns of the perovskite/YSZ mixtures after annealing at 1300°C for 120 h are shown in Fig. 1(a)–(d), for La, Pr, Nd and Gd manganites, respectively. The reaction products identified, are listed in Table 1. The main reaction product in the case of the La, Pr and Nd Sr-free manganites was the pyrochlore $RE_2Zr_2O_7$. The extent of its formation is reduced as the ionic radius of the rare earth cation decreases in the order Pr > Nd, while for Gd (with even lower ionic radius), no $Gd_2Zr_2O_7$ formation could be identified. The amount of $La_2Zr_2O_7$ formed, was lower than that of $Pr_2Zr_2O_7$ and $Nd_2Zr_2O_7$, even though $La^{3+}$ is larger than the other rare earth cations. Sr-doping suppresses the formation of the pyrochlore product. Thus, for 15 mol% Sr, only small amounts of $Pr_2Zr_2O_7$ and $Nd_2Zr_2O_7$ were identified, while for 30 mol% Sr there was no pyrochlore formation. As Sr content increases, the formation of $SrZrO_3$ reaction product is favored. However, the extent of its formation is different. The amount of $SrZrO_3$ was semiquantitatively evaluated by dividing the area of its major peak in the XRD pattern by that of YSZ. The results are plotted in Fig. 2 as a function of Sr content for the rare earth manganites of this study. As can be seen, the amount of $SrZrO_3$ formed, increases with increasing Sr content, and with decreasing rare earth ionic radius. In the XRD patterns of the perovskite/YSZ mixtures [Fig. 1(a)–(d)], the formation of $Mn_3O_4$ can be observed for the samples that exhibit high reactivity with YSZ.

## 4 Discussion

The reaction of $RE_{1-x}Sr_xMnO_{3\pm\delta}$ with YSZ can be described by the following general equation:

$$\begin{aligned} & RE_{1-x}Sr_xMnO_{3\pm\delta} + (a+b)ZrO_2 \\ & \quad = RE_{1-x-a}Sr_{x-b}MnO_{3\pm\delta} \qquad (1) \\ & \quad + a/2RE_2Zr_2O_7 + bSrZrO_3 \end{aligned}$$

The amount of $Y_2O_3$ is small, and it does not take part to the reaction, since no yttrium containing products were identified. Which of the two reaction products appearing in eqn (1) is formed, depends

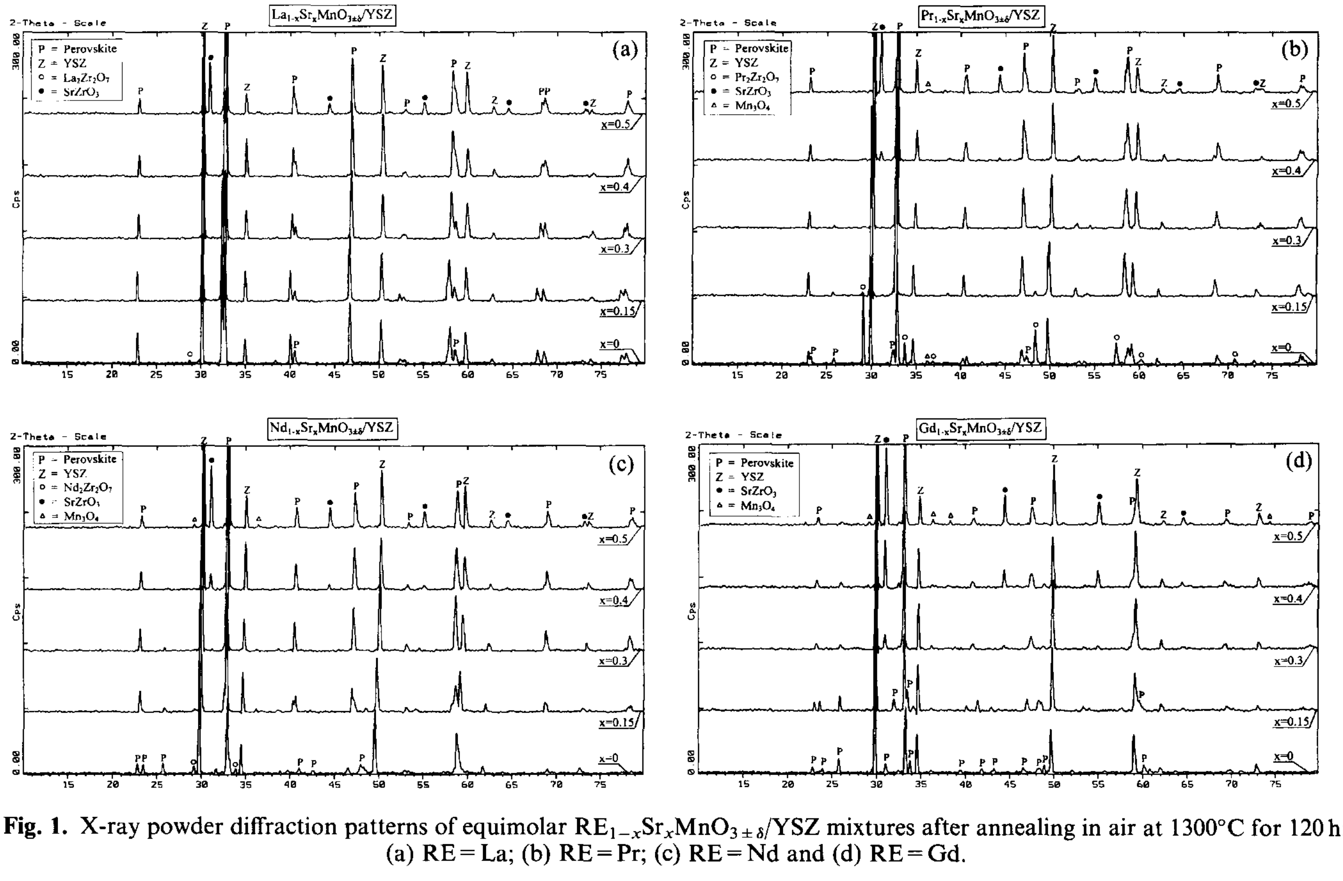

Fig. 1. X-ray powder diffraction patterns of equimolar $RE_{1-x}Sr_xMnO_{3\pm\delta}$/YSZ mixtures after annealing in air at 1300°C for 120 h: (a) RE = La; (b) RE = Pr; (c) RE = Nd and (d) RE = Gd.

**Table 1.** Reaction products identified by XRD in equimolar perovskite/YSZ powder mixtures after annealing at 1300°C for 120 h

| *Composition*[a] | *Reaction product identified by XRD values in parentheses are $I_{product}/IYSZ$ (%)* | *Remarks* |
|---|---|---|
| LSM-0 | $La_2Zr_2O_7$ (2·0) | |
| LSM-15 | | No reaction products |
| LSM-30 | | No reaction products |
| LSM-40 | | No reaction products |
| LSM-50 | $SrZrO_3$ (37·7) | |
| PSM-0 | $Pr_2Zr_2O_7$ (65·5) | Small amount of $Mn_3O_4$ |
| PSM-15 | | Small amount of $Pr_2Zr_2O_7$ |
| PSM-30 | | No reaction products |
| PSM-40 | $SrZrO_3$ (6·6) | |
| PSM-50 | $SrZrO_3$ (46·4) | Small amount of $Mn_3O_4$ |
| NSM-0 | $Nd_2Zr_2O_7$ (5·4) | |
| NSM-15 | | Small amount of $Nd_2Zr_2O_7$ |
| NSM-30 | | No reaction products |
| NSM-40 | $SrZrO_3$ (8·6) | |
| NSM-50 | $SrZrO_3$ (62·6) | Amount of $Mn_3O_4$ slightly greater than in PSM-50 |
| GSM-0 | | No reaction products (no $Gd_2Zr_2O_7$ formation) |
| GSM-15 | | No reaction products |
| GSM-30 | $SrZrO_3$ (7·3) | |
| GSM-40 | $SrZrO_3$ (30·0) | Small amount of $Mn_3O_4$ |
| GSM-50 | $SrZrO_3$ (67·9) | Amount of $Mn_3O_4$ greater than in other samples |

[a] LSM-0, LSM-15, ... , refers to compositions of $La_{1-x}Sr_xMnO_{3\pm\delta}$ with 0, 0·15, ... , mol% Sr, respectively. LSM, PSM, NSM and GSM refers to La, Pr, Nd and Gd manganites, respectively.

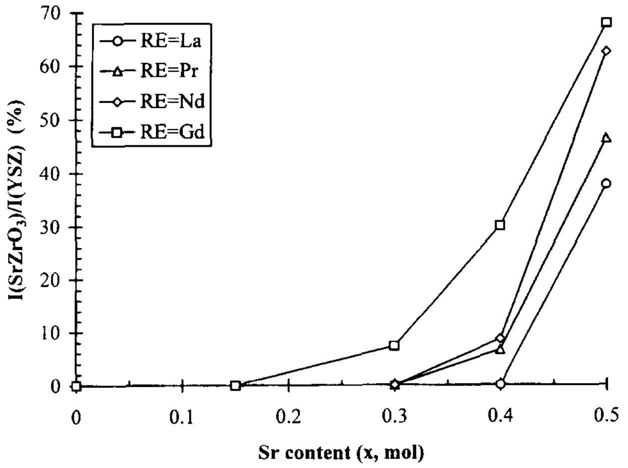

**Fig. 2.** Ratio of areas of the major XRD peaks of $SrZrO_3$ and YSZ as a function of Sr content for $RE_{1-x}SrMn_{3\pm\delta}$/YSZ powder mixtures after annealing at 1300°C for 120 h.

on the Sr content of the perovskite. For Sr-free or low Sr-containing compositions the formation of $RE_2Zr_2O_7$ is favored, whereas for high Sr-content, $SrZrO_3$ is formed.

The extent of pyrochlore $RE_2Zr_2O_7$ formation is expected to be a function of its stability. The enthalpy of formation of $RE_2Zr_2O_7$ decreases with decreasing ionic radius of the rare earth cation.[7] Therefore, the stability of the pyrochlore is reduced in the order $La_2Zr_2O_7 > Pr_2Zr_2O_7 > Nd_2Zr_2O_7 > Gd_2Zr_2O_7$. As a result, the amount of the pyrochlore formed after annealing, was shown to decrease in the same order, the only exception being $La_2Zr_2O_7$, which even though it is the most stable, forms only in minor amounts. The reason for this, may be found in the fact that $LaMnO_{3\pm\delta}$ has a more stable perovskite structure. Pr, Nd and Gd manganites have an orthorhombic structure,[8-10] that exhibits a more severe distortion from the ideal cubic perovskite. La manganite, on the other hand, has a rhombohedral structure,[11] whose deviation from the ideal perovskite is smaller than for the other rare earth manganites, due to the larger $La^{3+}$ cation.

The reaction product $SrZrO_3$ is formed in the case of compositions with high Sr content. As the same product is formed irrespective of the rare earth cation involved, the reason for the different extent of $SrZrO_3$ formation can be found by examining the relative stability of the rare earth manganites. The compositions $RE_{0.5}Sr_{0.5}MnO_{3\pm\delta}$, may be considered to consist of $REMnO_{3\pm\delta}$ and $SrMnO_3$, in equal molar amounts. Therefore, without loss of generality, we can compare the relative stability of $REMnO_{3+\delta}$ oxides. An empirical correlation has been derived by Yokokawa *et al.*[12] between the enthalpy of formation ($\Delta_r H^\circ$) of perovskite compounds from binary oxides, and the tolerance factor (t). In the case of $A^{III}B^{III}O_3$ oxides, the correlation is:[12]

$$\Delta_r H^\circ = -90 + 720(1 - t)\mathrm{kJ\,mol^{-1}} \qquad (2)$$

where the tolerance factor, $t$, can be evaluated from Shannon's[13] ionic radii as

$$t = \frac{r_A(\mathrm{XII}) + r_o}{\sqrt{2}(r_B(\mathrm{VI}) + r_o)} \qquad (3)$$

where $r_A(XII)$, $r_B(VI)$ and $r_O$ are ionic radii for A-site cations in 12-coordination, B-site cations in 6-coordination and oxide ions, respectively. The tolerance factors of the rare earth manganites of this study were calculated using eqn (3), and their $\Delta_r H^\circ$ values were estimated by eqn (2). Figure 3 shows $\Delta_r H^\circ$ as a function of $1-t$ for $REMnO_3$ (RE = La, Pr, Nd, Gd). As can be seen, the stability of the manganites decreases with decreasing $t$. As a result, $SrZrO_3$ is formed in greater amounts as the tolerance factor of the manganites decreases, and therefore, as the deviation from the ideal cubic perovskite structure increases.

With decreasing Sr concentration in the perovskite due to the formation of $SrZrO_3$, according to eqn (1), the A-site substoichiometry of the perovskite is enhanced. Thus, the activity of B-site Mn cations becomes larger compared with that of the A-site cations. As a result, manganese ions start to precipitate as a compound with lower valence state, namely $Mn_3O_4$. This observation is in agreement with the chemical equilibria calculations of Yokokawa *et al.*[3] The formation of $Mn_3O_4$ is more noticeable for the perovskite compositions with 50 mol% Sr, which show the greatest reactivity with YSZ. In the case of $La_{0.5}Sr_{0.5}MnO_{3\pm\delta}$ though, no $Mn_3O_4$ formation could be identified. This may be attributed to the lower reactivity of lanthanum strontium manganite (less $SrZrO_3$ formed), and to its more stable perovskite structure, which has a greater capacity to retain an A-site substoichiometry. A small amount of $Mn_3O_4$ was formed in the case of $PrMnO_{3\pm\delta}$, due to its high reactivity towards $Pr_2Zr_2O_7$ formation. The decrease of the Pr concentration in the perovskite, again results in an enhancement of the A-site substoichiometry, according to eqn (1), and therefore, to the precipitation of $Mn_3O_4$.

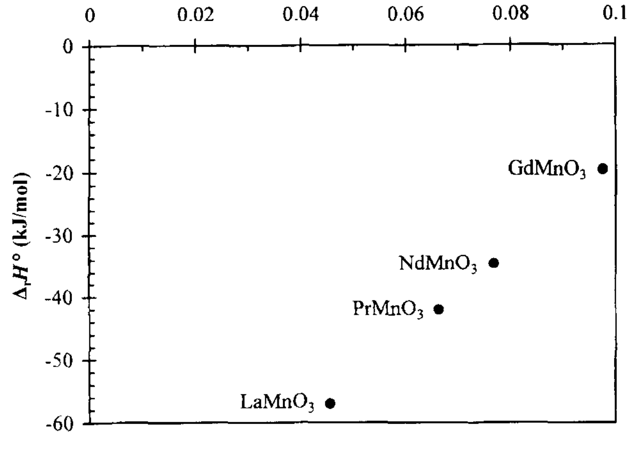

**Fig. 3.** Enthalpy of formation from binary oxides for $REMnO_3$ (RE = La, Pr, Nd, Gd), estimated from eqn (2), as a function of $1-t$.

The reactivity of $La_{1-x}Sr_xMnO_{3\pm\delta}$ oxides of this study appears to be lower than that found in other studies.[12] This is attributed to the reduced Zr-activity in the YSZ electrolyte used in this work (90 mol% $ZrO_2$), compared to the Zr-activity in YSZ used in the other studies (reported 92 mol% $ZrO_2$). Therefore, the use of YSZ electrolyte with less $ZrO_2$ content is a possible way of reducing the extent at which the undesirable reaction products are formed. Other ways for improving the cathode/electrolyte chemical compatibility include the use of low fabrication temperatures and the preparation of La-deficient perovskites.[1,2,14]

## References

1. van Roosmalen, J. A. M. and Cordfunke, E. H. P., Chemical reactivity and interdiffusion of $(La,Sr)MnO_3$ and $(Zr,Y)O_2$ solid oxide fuel cell cathode and electrolyte materials. *Solid State Ionics*, 1992, **52**, 303–312.
2. Stochniol, G., Syskakis, E. and Naoumidis, A., Chemical compatibility between strontium-doped lanthanum manganite and yttria-stabilized zirconia. *J. Am. Ceram. Soc.*, 1995, **78**, 929–932.
3. Yokokawa, H., Sakai, N., Kawada, T. and Dokiya, M., Thermodynamic analysis on interface between perovskite electrode and YSZ electrolyte. *Solid State Ionics*, 1990, **40/41**, 398–401.
4. Poulsen, F. W. and van der Puil, N., Phase relations and conductivity of Sr- and La-zirconates. *Solid State Ionics*, 1992, **52–53**, 777–783.
5. Ishihara, T., Kudo, T., Matsuda, H. and Takita, Y., Doped $PrMnO_3$ perovskite oxide as a new cathode of solid oxide fuel cells for low temperature operation. *J. Electrochem. Soc.*, 1995, **142**, 1519–1524.
6. Blank, D. H. A., Kruidhof, H. and Flokstra, J., Preparation of $YBa_2Cu_3O_{7-\delta}$ by citrate synthesis and pyrolysis. *J. Phys. D*, 1988, **21**, 226–237.
7. Bolech, M., Cordfunke, E. H. P., van Genderen, A. C. G., van der Laan, R. R., Janssen, F. J. J. G. and van Miltenburg, J. C., The heat capacity and derived thermodynamic functions of $La_2Zr_2O_7$ and $Ce_2Zr_2O_7$ from 4 to 1000 K. *J. Phys. Chem. Solids*, 1997, **58**, 433–439.
8. Kostogloudis, G. Ch., Vasilakos, N. and Ftikos, Ch., Preparation and characterization of $Pr_{1-x}Sr_xMnO_{3\pm\delta}$ ($x = 0$, 0·15, 0·3, 0·4, 0·5) as a Potential SOFC cathode material operating at intermediate temperatures (500–700°C). *Journal of the European Ceramic Society*, 1997, **17**, 1513–1521.
9. Kostogloudis, G. Ch. and Ftikos, Ch., Characterization of $Nd_{1-x}Sr_xMnO_{3\pm\delta}$ cathode materials for intermediate temperature operation. Submitted for publication in *J. Solid State Chem.*
10. Kostogloudis, G. Ch. and Ftikos, Ch., Effect of Sr-doping on the structural and electrical properties of gadolinium manganite. Submitted for publication in *J. Mater. Sci.*
11. Hammouche, A, Siebert, E. and Hammou, A., Crystallographic, thermal and electrochemical properties of the system $La_{1-x}Sr_xMnO_3$ for high temperature solid electrolyte fuel cells. *Mat. Res. Bull.*, 1989, **24**, 367–380.
12. Yokokawa, H., Kawada, T. and Dokiya, M., Thermodynamic regularities in perovskite and $K_2NiF_4$ compounds. *J. Am. Ceram. Soc.*, 1989, **72**, 152–153.
13. Shannon, R. D., Revised effective ionic radii and systematic studies of interatomic distances in halides and chalcogenides. *Acta Cryst.*, 1976, **A32**, 751–767.
14. Minh, N. Q., Ceramic fuel cells. *J. Am. Ceram. Soc.*, 1993, **76**, 563–858.